Applied Physics B (2019) 125:92
https://doi.org/10.1007/s00340-019-7199-7

Applied Physics B
Lasers and Optics

Efficient Er:Ti:$LiNbO_3$ ridge waveguide amplifier by patterning As_2S_3 layer

K. Ahmadi[1] · A. Zakery[1] · G. M. Parsanasab[2]

Received: 1 February 2019 / Accepted: 24 April 2019 / Published online: 6 May 2019

Abstract
In this study, the effect of As_2S_3 waveguide layer on propagation gain for Er:Ti:$LiNbO_3$ ridge waveguide amplifiers is investigated. In comparison with a typical titanium in-diffused channel waveguide, the three side Erbium in-diffusion of a 6 µm wide ridge waveguide and the better light confinement has improved the overlap between Er concentration and guided mode profiles up to 2.58 times. Our simulation demonstrates that by purposely adjusting the thickness of the three side As_2S_3 layer it is possible to pull the guided mode towards the ridge/air interface where Er concentration is higher. Consequently in this new configuration by taking advantage of the high refractive index As_2S_3 layer and mode de-shaping, the overlap relative to a ridge free of As_2S_3 layer has increased by 1.5 times thereby gain coefficient has been improved from 3.2 to 4.28 dB/cm at a coupled pump power of 200 mW. In comparison with a typical Ti channel waveguide amplifier, the relative overlap has increased by 3.88 times resulting in noticeable gain improvement from 0.65 to 4.28 dB/cm under the same Er diffusion conditions.

1 Introduction

Over the past decades $LiNbO_3$ has been the material of choice for integrated optics applications due to its high electro-optic, acousto-optic and nonlinear optical coefficients. Furthermore, optical channel waveguides as basic building blocks in integrated photonics are fabricated by titanium in-diffused or proton exchange well-established methods leading to development of efficient photonic elements such as switches, modulators and when doped with rare earth ions, waveguide amplifiers and lasers. In particular, over the past decades Er-doped $LiNbO_3$ waveguide amplifiers have attracted considerable interest in integrated circuits when optically pumped by 980 or 1480 nm radiation capable of amplification and lasing at third telecommunication wavelength around 1.55 µm [1]. In these kinds of waveguide amplifiers, the overlap integral between Er profile and optical mode which is related to the optical gain is low so there have been much effort to improve it which plays a determining role in enhancing optical gain [2]. All the research carried out on Er doped Ti channel waveguide amplifiers has led to the measured small-signal gain values of 1.7 dB/cm (net gain) [3] and 2 dB/cm (internal gain) [4] pumped at 980 nm and 1480 nm, respectively. Net, internal and propagation gain is defined elsewhere [5].

To enhance propagation gain it is required to pull guided modes towards the surface where in-diffused surface Er concentration is higher thereby overcoming propagation loss to achieve high enough optical gain and make integrated lasers [6] [7]. As_2S_3 layer due to its high nonlinear coefficient, low thermal loss and low processing temperature when combined with ferroelectric $LiNbO_3$ crystal has further potential applications in integrated photonics such as Mach–Zehnder interferometers and microring resonators [8–10]. High refractive index materials As_2S_3 and TiO_2 as cladding layers were two candidates for which their higher refractive indices around 2.4 at 1.55 µm compared to air lead to gain enhancement [11]. Song et al. reported that the optical gain has been enhanced from 1.1 to 2 dB/cm by utilizing the patterned As_2S_3 overlay [12].

On the other hand, ridge waveguides have more advantages compared to conventional guides such as lower bending loss, strong mode confinement that makes them a better choice in nonlinear frequency converters, electro-optic modulators. There has been a variety of methods for fabricating

✉ A. Zakery
zakeri@susc.ac.ir

[1] Physics Department, College of Sciences, Shiraz University, Shiraz 71946-24795, Iran

[2] Electrical Engineering Faculty, Shahid Beheshti University, Velanjak, Tehran 14966-47535, Iran

ridge waveguide structures on $LiNbO_3$ to decrease sidewall scattering losses bellow 1 dB/cm [13, 14], in which employing a blade diamond (optical grade dicing) has emerged as a powerful technique to fabricate low loss < 0.2 dB/cm ridge waveguides. Recently Suntsov et al. reported for the first time an internal gain of 2.7 dB/cm for the coupled pump power of 200 mW at 1486 nm by a new technique utilizing optical grade dicing and three side Er and Ti diffusion at high temperatures [15, 16].

In this context, we proceed with the simulation of gain improvement for TM polarization in the ridge waveguide structure using the benefits of As_2S_3 layer to elevate signal mode near to three sides of the waveguide where the higher Er concentration yields an improved propagation gain. First, we take a look at analytical gain expressions to define propagation gain in dB/cm then it has been shown that a three side Er in-diffused ridge waveguide of 6 μm width has the best overlap resulting in more signal enhancement as ridge width increases. Finally, the effect of As_2S_3 layer thickness on the behavior of propagation gain is numerically considered and the optimal top and sidewall As_2S_3 thicknesses for the best amplifier performance are evaluated.

2 Analytical expressions

To model Er-doped $LiNbO_3$ waveguide amplifiers some assumptions are to be made bellow.

1. It can be modeled by a two level atomic model if the 1480 nm pump wavelength is used where only upper level $4I_{13/2}$ and ground level $4I_{15/2}$ of the energy level of Er^{3+} in $LiNbO_3$ are involved [17–19].
2. The other good approximation is to neglect the excited state absorption which only affects the pump absorption along the waveguide. Some other effects like Er-ion pairing and $LiNbO_3$ background impurity loss is small [17–19].
3. At the gain region higher than 20 dB, amplified spontaneous emission noise (ASE) can significantly reduce the gain due to saturation, therefore, ASE evolution in this kind of waveguide amplifier is usually ignored and moreover for high pump powers (above 20 dBm), the population inversion is maximized so that gain is considered to be uniform along the propagation direction of amplifier [18], [20].

In the two-level model of Erbium-doped $LiNbO_3$ waveguide amplifiers and lasers pumped by 1480 nm radiation, propagation equation for describing the evolution of signal power along the waveguide in steady state is given by [2, 21]:

$$\partial P_s(z)\big/\partial z = \big(\gamma_{21} - \gamma_{12}\big)P_s(z) - \alpha P_s(z), \tag{1}$$

$$\gamma_{21} = N_2(z) \iint_A \psi_s(x,y)\sigma_s^e \rho Er(x,y)\mathrm{d}x\mathrm{d}y, \tag{2}$$

$$\gamma_{12} = N_1(z) \iint_A \psi_s(x,y)\sigma_s^a \rho Er(x,y)\mathrm{d}x\mathrm{d}y, \tag{3}$$

where P_s is the signal power, ρ the density of Erbium atoms at the $LiNbO_3$ surface, $\psi_s(x,y)$ and $\mathrm{Er}(x,y)$ are normalized signal mode distribution and Erbium concentration profile. σ_s^e and σ_s^a are cross sections for stimulated emission and absorption at the signal wavelength. $N_1(z)$ and $N_2(z)$ are fraction of Erbium atoms in the ground and excited states, respectively ($N_1(z) + N_2(z) = 1$ [21]) and are determined by the pump efficiency.

After substituting (2) and (3) in (1) it becomes

$$\frac{1}{P_s(z)}\frac{\partial P_s(z)}{\partial z} = \rho\Gamma\left[\left(\sigma_s^e + \sigma_s^a\right)N_2(z) - \sigma_s^a\right] - \alpha_s, \tag{4}$$

$$\Gamma = \iint_A \psi_s(x,y)\mathrm{Er}(x,y)\mathrm{d}x\mathrm{d}y. \tag{5}$$

Here Γ is defined as the overlap integral between the mode distribution and Er concentration profile over the waveguide cross section. Here $\psi_s(x,y)$ and $\mathrm{Er}(x,y)$ are normalized such that Γ takes a value between zero and one. It is clear that the higher Γ and ρ the higher the propagation gain while the parameter Γ for typical channel waveguide is less than 0.2 where surface in-diffused Er profile described by the Fick type diffusion is approximated by a Gaussian function. By inserting the conversion factor $10\log(e)$ into Eq. 4 the propagation gain defined as the gain relative to non Er-doped waveguide which has loss α_s (decibel per unit length) is given by

$$\text{Gain (dB/cm)} = 10\log(e)\rho\Gamma\left[\left(\sigma_s^e + \sigma_s^a\right)N_2(z) - \sigma_s^a\right]. \tag{6}$$

3 Simulation results

3.1 Ridge waveguide amplifier

To study the gain behavior under the effect of an As_2S_3 layer deposited on an Er-doped Ti:$LiNbO_3$ ridge waveguide structure of 6 μm width we have used 3-cm *x*-cut and *y*-propagation $LiNbO_3$ samples. Our proposed structure presented schematically in Fig. 1 is an *x*-cut and *y*-propagation Ti in-diffused $LiNbO_3$ ridge waveguide of 6 μm width and 15 μm height with an As_2S_3 layer deposited on each of the three sides. The fabrication process has been illustrated schematically in Fig. 2. The wafer is spin coated with a positive

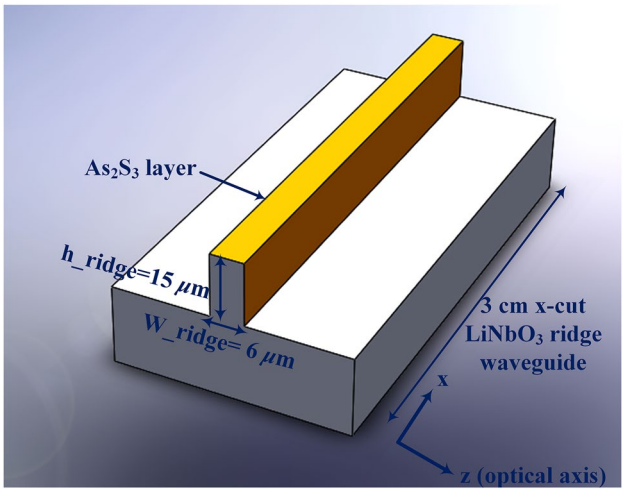

Fig. 1 Er:Ti:$LiNbO_3$ ridge waveguide structure with As_2S_3 layer deposited from three sides

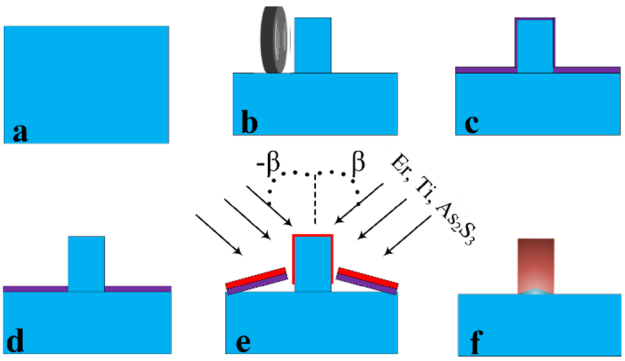

Fig. 2 A schematic of three side Er, Ti, As_2S_3 deposition. **a** *x*-cut $LiNbO_3$ wafer, **b** ridges cut into the substrate, **c–d** photoresist spin coating and developing, **e–f** three side deposition of Ti(Er), lift-off and finally in-diffusion. The steps from **c** to **e** is repeated for deposition of As_2S_3

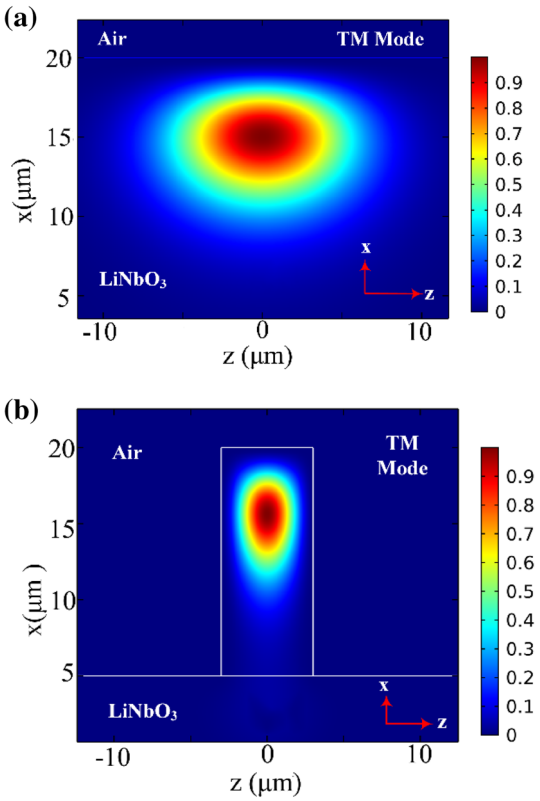

Fig. 3 Normalized mode intensity profile. **a** TM mode for a typical channel waveguide, **b** TM mode for a ridge waveguide. *Z* axis denotes the optical axis direction

photoresist after the fabrication of ridge structure by precision wafer dicing, see Fig. 2a–c. Then the sample is exposed to UV radiation for a short time and developed subsequently as shown in Fig. 2d. Next, evaporation of Er and Ti at the appropriate angle, lift off and diffusion processes under the diffusion conditions given in the following are done, Fig. 2e–f. Finally, As_2S_3 layer is deposited by repeating the steps (c–f) in Fig. 2.

There are two reasons why we focused on TM polarization in gain simulation. First, As_2S_3 ring resonators coupled to Ti:$LiNbO_3$ channel waveguide by side coupling and top coupling have been designed to function with TM polarization to implement filtering function efficiently [9] [10]. Second, not only Er ions absorption at 1480 nm and emission at signal wavelength 1531 nm in Er-doped amplifiers are highly σ-polarized which corresponds to TM mode for *x*-cut $LiNbO_3$ wafers but also there is a better overlap with Er profile yielding more optical gain than the TE mode [12].

To perform simulations, we have used the mode analysis method of commercial COMSOL software to solve for optical modes and calculate the overlap coupling between optical modes and Er concentration, overlap pump-related integrals which are required for optical gain calculation in Er-doped $LiNbO_3$ ridge waveguides. We computed the TM guided mode and Er concentration profiles based on Er/Ti anisotropic temperature-dependent diffusion coefficient in a single-mode channel waveguide defined in an *x*-cut $LiNbO_3$ wafer by the mode analysis module. Our Calculations show that for a waveguide with 100 nm Ti thickness and 6 μm width in-diffused at 1060 °C for 10 h a single mode waveguide is achieved at 1460 nm $< \lambda <$ 1560 nm having the best overlap with pump and Er concentration. While for the ridge structure, a time of 3.7 h has been considered for diffusion of the same Ti thickness to provide a more symmetric guided mode in the depth direction of the ridge as shown in Fig. 3. In the case of a ridge structure, this choice not only helps to utilize the larger diffusion coefficient of Er in the *z*-axis perpendicular to the ridge side walls (about 1.3 times) but also promotes the three side Er diffusion and hence the optical

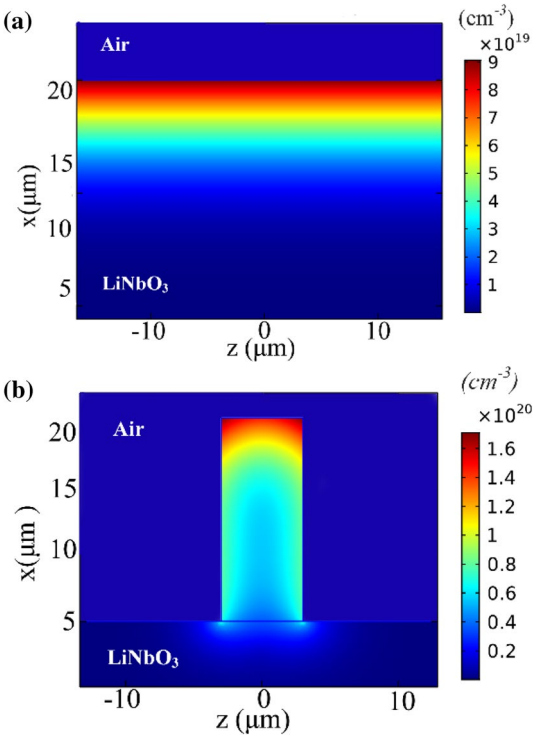

Fig. 4 Er concentration profile. **a** Typical channel waveguide, **b** a ridge waveguide of 6 μm width

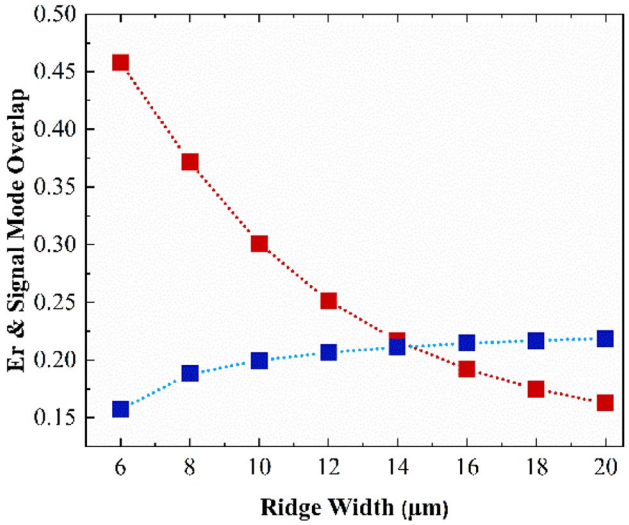

Fig. 5 Er & mode overlap vs ridge width. Red square diagram shows the overlap for three side Er in-diffusion and blue square for top only Er in-diffusion

gain. It should be noted that in gain spectrum of Er doped amplifiers the gain coefficient at 1531 nm is higher.

Therefore, gain evolution has been determined for the signal wavelength of 1531 nm under 1480 nm pumping in which there is a better overlap than 980 nm wavelength at which there are some drawbacks [22].To model the small-signal gain other parameters namely the fluorescence lifetime, the absorption and emission cross-sections for pump and signal wavelength are (for TM polarization) [2]:

$$\tau = 2.63 \text{ ms}, \sigma_{\text{p}}^{\text{a}} = 3.1e-24 \text{ cm}^2, \sigma_{\text{p}}^{\text{e}} = 0.1e-24 \text{ cm}^2,$$
$$\sigma_{s}^{a} = 2.54e-24 \text{ cm}^2, \sigma_{\text{s}}^{\text{e}} = 2.4e-24 \text{ cm}^2.$$

Previous results demonstrate that for Er layers evaporated at different angles, the 11 nm Er deposited at the angle of $\pm 60°$ with respect to the substrate normal gives more internal gain when pumped at a coupled power of 200 mW [15] using the geometry shown in Fig. 1. According to angle deposition formula for thickness calculation, evaporation at $\pm 60°$ yields a ratio of 11/9.5 between the top layer thickness and sidewalls for 11 nm Er layer which has been considered in simulation. We simulated the two dimensional Er profile with the time-dependent diffusion module of COMSOL as well. The Er profile of a ridge and typical channel waveguide has been illustrated in Fig. 4. The legend represents higher Er concentration (1.8e20 cm^{-3}) than (0.9e20 cm^{-3}) for the typical channel waveguide. The simulation results show that for Er concentration up to 2e20 cm^{-3} pumped at 200 mW the waveguide amplifier shows a linear relation between gain and length up to 10 cm [15].

Let us now consider the advantage of three side Er in-diffusion against the top only case as a function of ridge width. For top only case as the width increases from 6 to 20 μm the intensity profile is extended horizontally and pulled more towards the top interface which means both overlaps are improved from 0.15 to 0.22 as shown in Fig. 5 and higher Er ions are available so that gain improves. The gradual behavior in gain improvement is attributed to the decrease in relative intensity as the width increases. While for three side Er in-diffused ridge waveguides the narrowest width of 6 μm has demonstrated the best overlap and gain performance. This is because for the sidewall Er in-diffused case the diffusion length perpendicular to the ridge sidewalls is about 5.1 μm which not only matches better the signal profile but also mode intensity is higher. It means a significant Γ and more optical gain results as shown in Figs. 5, 6. Therefore, the choice of a 6 μm wide ridge waveguide with Er deposited from three sides represents the best waveguide amplifier performance. It is worth to note that such ridge waveguides will offer more flexibility in terms of deposition of a high refractive index material at an angle with respect to the substrate normal to purposely adjust the layer deposition thickness according to gain enhancement modelling as it will be considered in the following section.

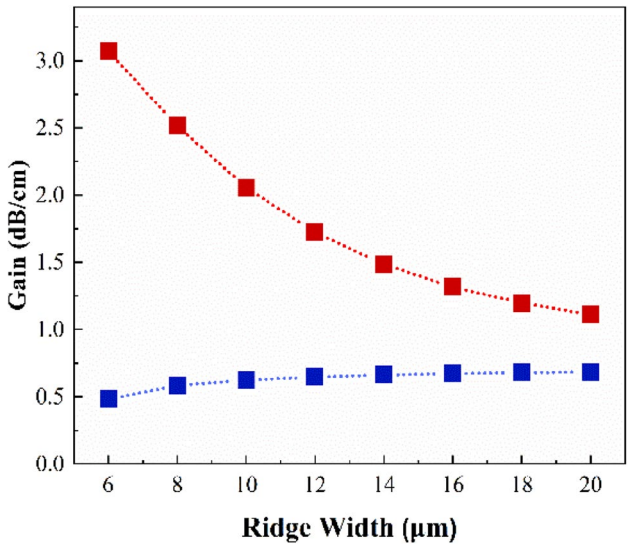

Fig. 6 Propagation gain vs ridge width. Red square diagram represents the gain calculation results for three side Er in-diffusion and blue square for top only Er in-diffusion

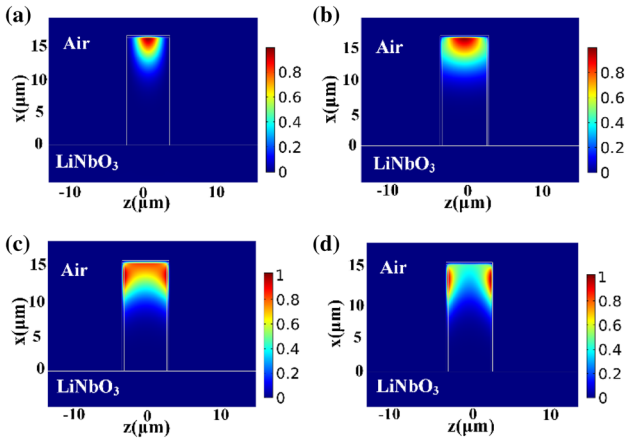

Fig. 7 Evolution of the TM mode intensity at 1.531 μm as a function of As_2S_3 sidewall thickness (h) at As_2S_3 top thickness of 360 (nm), **a** $h=25$ nm, neff = 2.2115, **b** $h=255$ nm, neff = 2.2139, **c** $h=275$ nm, neff = 2.2151, **d** $h=285$ nm, neff = 2.2161

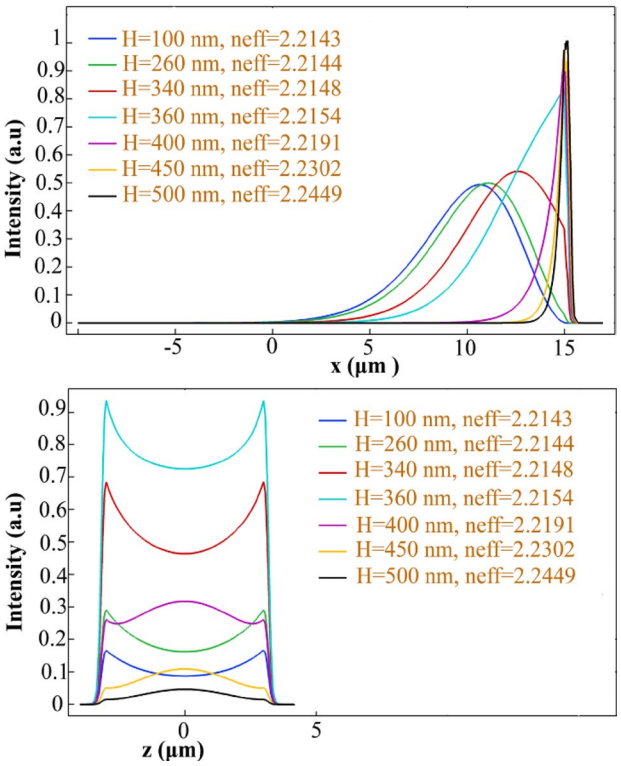

Fig. 8 The evolution of TM mode intensity along the ridge sidewall (z-axis) and along the width of the ridge (x-axis) vs As_2S_3 top thickness. H denotes the As_2S_3 top thickness and neff is effective refractive index

3.2 Optimization of ridge amplifier

To improve further the efficiency of the amplification of a ridge waveguide amplifier which depends on the overlap between Er concentration profile and pump/signal intensity distribution As_2S_3 layer is used. The plot of the three side Er diffusion for 11 nm Er evaporated at ± 60° is shown in Fig. 4. Er diffusivity in the horizontal direction is more than in the vertical direction so diffusion length in the horizontal direction is about 5.1 μm while this is 4.47 μm for vertical direction. As we see from Fig. 4 Er concentration profile simulated by diffusion module of COMSOL is similar to an arch-shaped profile such that concentration is higher on the top corners of the ridge, therefore, As_2S_3 layer thickness on top and sidewalls is adjusted to pull signal mode to the region of high impurity to take full advantage of the Er diffusion and mode overlap. The evolution of signal mode as a function of some sidewall thicknesses while its top layer is at 360 nm is illustrated in Fig. 7. To understand better the pulling effect of As_2S_3 layer on TM mode along the width and height of the ridge is illustrated in Fig. 8.

As_2S_3 as a high refractive index material not only enhances Er and mode overlap but also affects the overlap integral between pump-fiber and pump-signal modes through mode de-shaping, which shows its effect as an ineffective input pump power in gain calculations:

3.2.1 Relative overlap calculations

Figure 9 shows the relative improvement of Er concentration profile and mode intensity as a function of As_2S_3 top thickness. We normalized the overlap relative to the case where As_2S_3 top thickness is zero. As seen, the maximum relative overlap at As_2S_3 top thickness of 395 nm is 1.5 times and increasing the thickness further cause to decrease the overlap and consequently optical gain since there is no

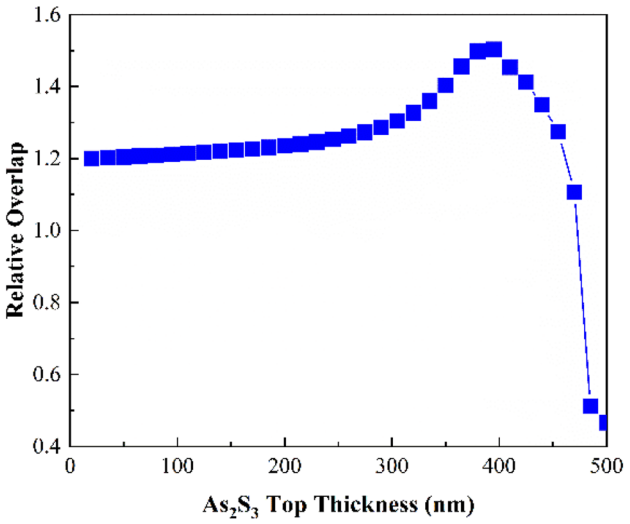

Fig. 9 Er profile and TM mode relative overlap vs As_2S_3 top thickness

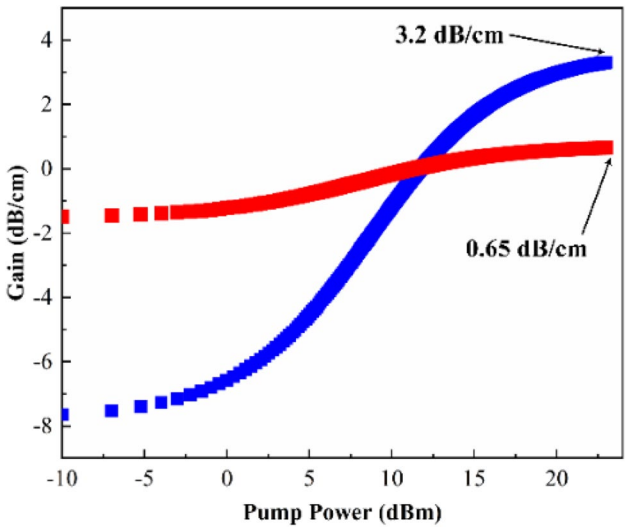

Fig. 10 Propagation gain vs pump power for Er:Ti:$LiNbO_3$ ridge (blue diagram) waveguide compared to channel Ti waveguide(red diagram)

Er ions available in As_2S_3 layer to be pumped and improve the gain further. Our simulation results show that overlap relative to a channel waveguide with the same Er diffusion parameters is about 3.88 at the optimum thickness of 395 nm.

3.2.2 Pump-related effects considerations

For As_2S_3 layer thicknesses above 300 nm mode de-shaping would happen significantly for which not only maximum Er concentration and mode overlap is obtained but also fiber-pump and pump-signal coupling must be considered in propagation gain calculations. The coupling integral between fiber, signal and pump is defined as follows [12]:

$$\eta_{\text{Signal \& Pump}} = \iint_A \psi_s(x,y)\psi_P(x,y)\mathrm{d}x\mathrm{d}y, \tag{7}$$

$$\eta_{\text{Pump \& Fiber}} = \iint_A \psi_P(x,y)\psi_F(x,y)\mathrm{d}x\mathrm{d}y, \tag{8}$$

where ψ_S, ψ_P and ψ_F are normalized signal, pump and fiber mode distributions, respectively. In fact, the overlap integral has changed the input pump power to the waveguide which means the waveguide is pumped ineffectively. By multiplying the overlap integrals and taking its product as the pump efficiency ratio, gain as a function of input pump power due to the As_2S_3 layer is calculated.

Figure 10 shows the gain evolution as a function of input pump power for a ridge waveguide without As_2S_3 overlay. The maximum obtainable gain coefficient at 200 mW pump power as shown is 3.28 dB/cm, whereas for a Ti channel counterpart with the same Er diffusion the maximum gain coefficient is 0.65 dB/cm. Indeed, the effective pump power which is a product of overlap integrals 7–8 and input pump power (200 mW) has decreased from 154 to 17.6 mW as the As_2S_3 top thickness increases from 0 to 500 nm so that the maximum gain which is defined as an effective gain coefficient is decreased from 3.2 to 0.4 dB/cm as illustrated in Fig. 13.

According to Eq. 6 by multiplying the effective gain Fig. 13 and relative Er and signal mode Fig. 9 the final simulated propagation gain is obtained, see Fig. 14. Having considered the relative Er and signal mode overlap (Fig. 10) and pump effects (Figs. 10, 11, 12, 13) it is found that gain coefficient is improved from 3.2 to 4.28 dB/cm at As_2S_3 top thickness of 350 nm and sidewall thickness of 275 nm. The ratio between As_2S_3 top and sidewalls thicknesses for the best amplification is realized at $\pm 54°$ evaporation angle. As we notice Er and mode overlap maximum occurs at As_2S_3 top thickness of 395 nm, as shown in Fig. 9 while the optimum thickness for gain is found to be 350 nm which is a large shift of −45 nm shown in Fig. 14 due to the stronger pump effects whereas this shift is −20 nm for Ti channel waveguide [12]. In Fig. 14 red square denotes the maximum gain attainable for a Ti channel standard waveguide to compare better the benefits of a ridge waveguide structure and a channel waveguide counterpart.

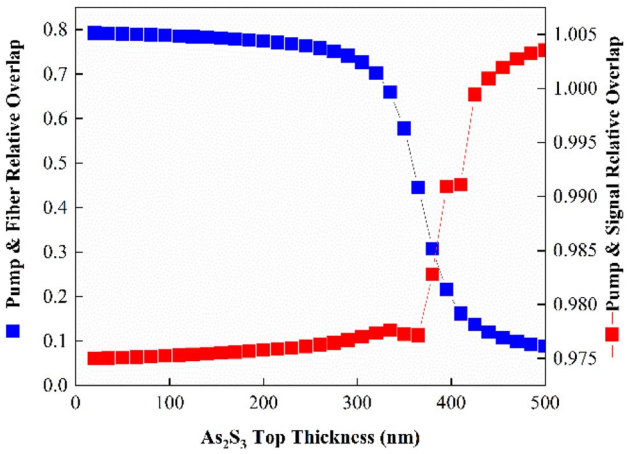

Fig. 11 Pump effects for TM mode in the ridge waveguide with As_2S_3 deposited from three sides. The data are normalized relative to the ridge waveguide without As_2S_3 layer

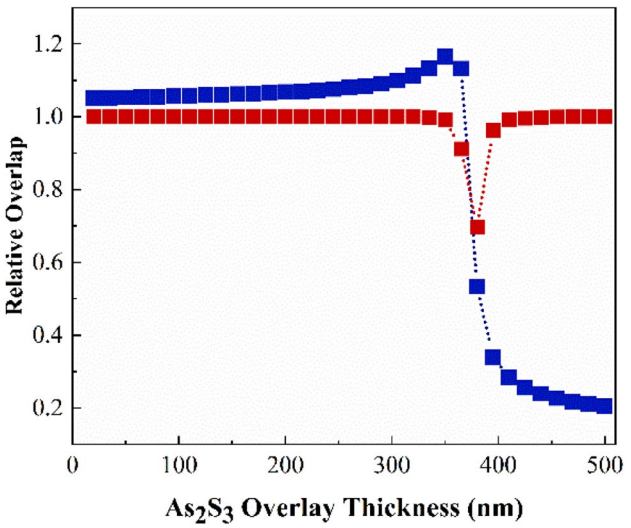

Fig. 12 Pump effects for TM mode in a channel waveguide. The data are normalized to the Ti channel waveguide without As_2S_3 overlay

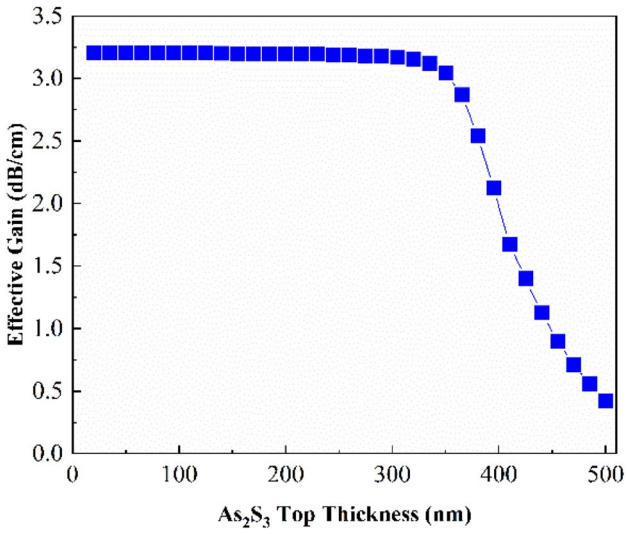

Fig. 13 Effective gain vs As_2S_3 top thickness for TM mode

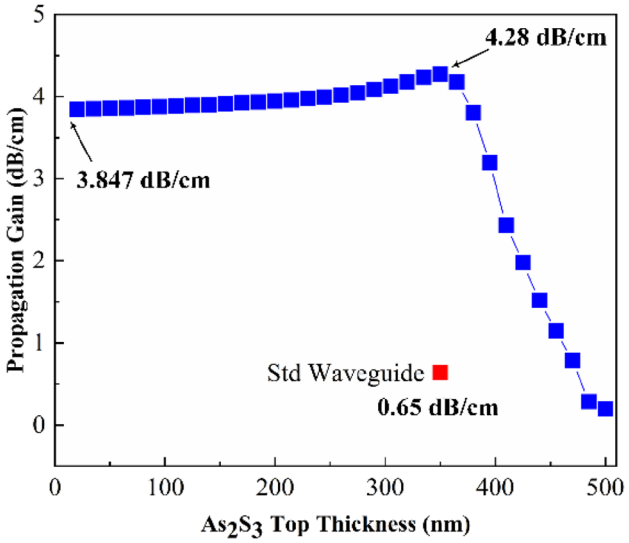

Fig. 14 Propagation gain vs As_2S_3 top thickness. Std denotes standard Ti channel waveguide. 3.847 and 4.28 dB/cm shows the improvement for As_2S_3 top thickness of 0 and 350 nm, respectively

4 Discussion

As_2S_3 layer has influenced the fiber and waveguide coupling by changing the shape of the waveguide mode for both pump and signal which must be considered in coupling loss. The coupling overlap between a SMF fiber-Ti channel waveguide and SMF fiber-ridge waveguide which is normalized to Ti channel and ridge structure without an As_2S_3 waveguide, respectively, has been shown in Figs. 11, 12. For a Ti standard waveguide as shown in Fig. 12 the relative coupling for TM mode at 280 nm optimum thickness is 1.14 (+0.57 dB) which shows an improvement compared to that of for a Ti channel waveguide without As_2S_3 overlay. This is because As_2S_3 layer decrease the TM mode size which has a larger mode size (vertical: 10.7 µm horizontal: 13.8 µm) than that of an SMF fiber so that matches better the fiber mode that has a MFD of 10.2 µm at 1531 nm thereby reducing coupling loss [12]. For the ridge waveguide, the relative coupling for TM mode is 0.57 (−2.3 dB) at optimum As_2S_3 top thickness of 350 nm which increases the coupling loss. To decrease the high coupling loss the proposal is to use tapered As_2S_3 layer at the input and output ports to ensure that waveguide mode at the ends is the same to the normal ridge waveguide.

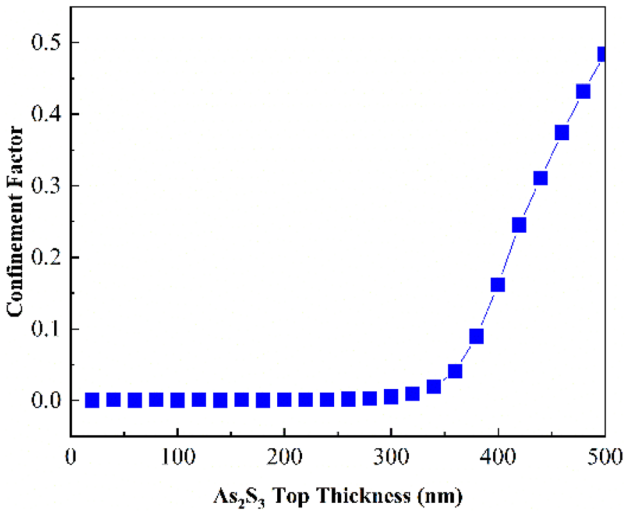

Fig. 15 Confinement factor in three side As_2S_3 layers for TM mode at 1531 nm signal wavelength

By sweeping the thickness of As_2S_3 layer on top of the ridge from 0 to 500 nm while the thickness on the sidewalls was 275 nm, it is observed in Fig. 15 that confinement factor which is the percentage of mode power in As_2S_3 layer for TM mode is increased up to 48% resulting in a steep decrease in optical gain as observed in Figs. 13, 14. In addition propagation loss due to the scattering will increase as the mode is pulled towards the ridge/As_2S_3 interface. To compensate for the propagation loss and even improve the optical gain further it is possible to introduce Er ions into As_2S_3 layer to add offsetting gain. Vu et al. demonstrated a complete loss compensation with 1480 nm pumping and a fully lossless waveguide with high nonlinear coefficient [21]. Such hybrid waveguide plays a key role in a number of important breakthrough experiments in nonlinear optics and telecommunications [23].

5 Conclusions

To summarize, ridge waveguide amplifier structures compared to channel counterparts will provide the advantage of three side Er/Ti diffusion allowing for higher active ions concentration and improved overlap between Er ions and mode intensity profiles. As our simulation results demonstrate ridge waveguide amplifiers will benefit from higher refractive index of As_2S_3 waveguide layer by pulling TM signal mode towards the ridge/As_2S_3 interface where Er concentration is higher so that optical gain is improved. The propagation gain coefficient has increased from about 3.2 to 4.28 dB/cm relative to a ridge waveguide free of As_2S_3 layer while the improvement is from 0.65 dB/cm to 4.28 dB/cm relative to a Ti in-diffused channel waveguide under the same diffusion conditions. Taking into account the typical propagation loss (0.4 dB/cm) and coupling loss for TM mode at 1531 nm (mode shape mismatch loss: 2.3 dB per facet, Fresnel loss per facet: 0.15 dB) about 6.74 dB net gain is achievable. Pulling the signal mode towards the ridge/As_2S_3 interface would cause more scattering losses which is well known to severely impact the nonlinear optical processes in these waveguides, therefore, introducing Er ions into As_2S_3 layer could make up for the propagation losses which is attributed to scattering losses.

References

1. R.G. Hunsperger, *Integrated optics: theory and technology* (Springer, Berlin, 2009)
2. M. Dinand, W. Sohler, IEEE J. Quantum Electron. **30**, 1267 (1994)
3. D.L. Zhang, F. Han, B. Chen, P.R. Hua, D.Y. Yu, E.Y.B. Pun, J. Lightwave Technol. **32**, 135 (2014)
4. R. Brinkmann, I. Baumann, M. Dinand, W. Sohler, H. Suche, IEEE J. Quantum Electron. **30**, 2356 (1994)
5. D.L. Zhang, P.R. Hua, E.Y.B. Pun, Opt. Commun. **279**, 64 (2007)
6. I. Baumann, R. Brinkmann, M. Dinand, W. Sohler, S. Westenhofer, IEEE J. Quantum Electron. **32**, 1695 (1996)
7. P. Becker, R. Brinkmann, M. Dinand, W. Sohler, H. Suche, Appl. Phys. Lett. **61**, 1257 (1992)
8. A. Zakery, S.R. Elliot, J. Non-Cryst. Solids **330**, 1 (2003)
9. Y. Zhou, X. Xia, W.T. Snider, J.H. Kim, Q. Chen, W.C. Tan, C.K. Madsen, IEEE Photonics Technol. Lett. **23**, 1195 (2011)
10. M.E. Solmaz, D.B. Adams, W.C. Tan, W.T. Snider, C.K. Madsen, Opt. Lett. **34**, 1735 (2009)
11. K. Kishioka, T. Kishimoto, K. Kume, IEICE Trans. Electron **E88-C**, 1041 (2005)
12. X. Song, W. Tan, W.T. Snider, X. Xia, C.K. Madsen, IEEE Photonics J. **3**, 686 (2013)
13. H. Hue, R. Ricken, W. Sohler, R.B. Wehrspohn, IEEE Photonics Technol. Lett. **19**, 417 (2007)
14. P. Rabiei, W.H. Steier, Appl. Phys. Lett. **86**, 161115 (2005)
15. S. Suntsov, C.E. Ruter, D. Kip, Appl. Phys. B **118**, 1234 (2017)
16. D. Brusk, S. Suntsov, C.E. Ruter, D. Kip, Opt. Express **25**, 29374 (2017)
17. A.A.M. Saleh, R.M. Jopson, J.D. Evankow, J. Aspell, IEEE Photonics Technol. Lett. **2**, 714 (1990)
18. C.R. Giles, E. Desurvire, J. Lightwave Technol. **9**, 271 (1991)
19. Y. Sun, G. Luo, J.L. Zyskind, A.A.M. Saleh, A.K. Srivastava, J.W. Sulhoff, Electron. Lett. **32**, 1490 (1996)
20. C.H. Huang, D.M. Gill, L. McCaughan, J. Lightwave Technol. **12**, 803 (1994)
21. Y. Sun, J.L. Zyskind, A.K. Srivastava, IEEE J. Sel. Top. Quantum Electron. **3**, 991 (1997)
22. C.H. Huang, L. McCaughan, IEEE J. Sel. Top. Quantum Electron. **2**, 367 (1996)
23. K. Vu, K. Yan, Z. Jin, X. Gai, D.-Y. Choi, S. Debbarma, B. Luther-Davis, S. Madden, Opt. Lett. **38**, 1766 (2013)